Neuropsychopharmacology (2003) 28, 1412–1421

www.neuropsychopharmacology.org

Dopamine Receptor Subtypes Selectively Modulate Excitatory Afferents from the Hippocampus and Amygdala to Rat Nucleus Accumbens Neurons

A Charara*[,1] and AA Grace[1]

[1]*Departments of Neuroscience and Psychiatry, University of Pittsburgh, Pittsburgh, PA, USA*

The nucleus accumbens (NAc) receives excitatory afferents from several cortical and limbic regions and dense dopaminergic inputs from the ventral tegmental area. We examined the effects of dopamine (DA) D1 and D2 selective drugs on the responses evoked in the NAc shell neurons recorded *in vitro* by stimulation of hippocampal and amygdaloid afferents. Activation of hippocampal and amygdaloid afferents induced excitatory postsynaptic responses that were depressed by bath application of DA in most of the cells recorded. The DA effect was substantially blocked by the D1 receptor antagonist SCH 23390, but not by the D2 receptor antagonist eticlopride. Moreover, the D1 receptor agonist SKF 38393, but not the D2 receptor agonist quinpirole, mimicked the effects of DA, although a small population of neurons exhibited a D1-mediated facilitation of the EPSP amplitude following fornix stimulation. These data demonstrate a DA receptor subtype-specific modulation of glutamatergic inputs to the NAc, with D1 agonists attenuating amygdaloid inputs, whereas hippocampal-evoked responses were either depressed or potentiated by D1 stimulation. Such facilitation or attenutation of hippocampal afferents against a background of suppression of other afferents would permit the hippocampus to have a dominant influence over behavior during periods of exploration.
Neuropsychopharmacology (2003) **28,** 1412–1421, advance online publication, 11 June 2003; doi:10.1038/sj.npp.1300220

Keywords: nucleus accumbens; dopamine; hippocampus; amygdala; afferents; *in vitro*

INTRODUCTION

The nucleus accumbens (NAc), which is the principal component of the ventral striatum, is central to the limbic system and is thought to play a role in the translation of limbic information into goal-directed behavior. Indeed, the NAc receives excitatory glutamatergic inputs primarily from limbic-related structures, including the hippocampus, basolateral amygdala (BLA), prefrontal cortex (PFC), and various thalamic nuclei (Sesack *et al*, 1989; Berendse and Groenewegen, 1990; Callaway *et al*, 1991; Pennartz *et al*, 1994; Finch, 1996). The NAc is also densely innervated by dopaminergic afferents originating in the ventral tegmental area (VTA) (Nauta *et al*, 1978). In many instances, these inputs converge on the same accumbal neurons (Sesack and Pickel, 1990, 1992; O'Donnell and Grace, 1995; Mulder *et al*, 1998). In turn, the NAc projects to areas involved in motor output such as the ventral pallidum, which influences several limbic-related thalamocortical circuits (Heimer and Alheid, 1991). A major target of the accumbens-ventral pallidal system is the mediodorsal nucleus of the thalamus (Lavin and Grace, 1994), which provides the major regulatory control over the PFC. The two main limbic input structures of the NAc can be assigned to distinct behaviors. The amygdala forms a link between sensory systems and structures involved in emotional behavior (Davis, 1992; Ledoux, 1993), whereas the hippocampus is important in memory tasks, particularly those involving spatial cues and context-dependent behaviors (Alvarez *et al*, 1995).

Dopaminergic neurotransmission within the NAc has received particular attention because of its role in promoting locomotion (Iversen, 1995), motivation and reward (Robbins and Everitt, 1996), and addiction and sensitization to drugs of abuse (Kalivas *et al*, 1993). Many behavioral studies have suggested that interactions between DArgic and glutamatergic inputs into the NAc contribute to this variety of psychomotor behaviors (Kalivas *et al*, 1993; Hyman, 1996; Robbins and Everitt, 1996). Ultrastructural studies of the NAc have found DArgic terminals apposed to both symmetrical and asymmetrical synapses (Sesack and Pickel, 1992), as well as a significant proportion unapposed to any postsynaptic structures (Bouyer *et al*, 1984;

*Correspondence: Dr A Charara, Department of Neuroscience, University of Pittsburgh, 446 Crawford Hall, Pittsburgh, PA 15260, USA, Tel: +1 412 624 8895, Fax: +1 412 624 9198,
E-mail: charara@brain.bns.pitt.edu
Received 14 January 2003; revised 01 April 2003; accepted 03 April 2003
Online publication: 28 April 2003 at http://www.acnp.org/citations/Npp042802022/default.pdf

Descarries *et al*, 1996). Thus, dopaminergic afferents to the NAc may modulate synaptic transmission either by releasing dopamine (DA) directly onto synapses or by causing a more diffuse increase in extracellular DA levels (Garris *et al*, 1994; Grace, 1991; Descarries *et al*, 1996).

Many electrophysiological studies have examined the effects of DA on synaptic transmission in the NAc. *In vivo* studies reported that VTA stimulation, DA iontophoresis, or DArgic drug administration reduced stimulus-evoked excitatory responses from either hippocampal or amygdaloid afferents (Yang and Mogenson, 1984; DeFrance *et al*, 1985; Yim and Mogenson, 1986, 1989; Floresco *et al*, 2001a, b). Moreover, studies using *in vitro* brain slice preparations of the NAc consistently demonstrated that DA and psychostimulants depress excitatory synaptic transmission (Pennartz *et al*, 1992b; Harvey and Lacey, 1996; O'Donnell and Grace, 1994). However, little is known regarding the relative contribution of D1- and D2-like receptors to the modulation of excitatory inputs from the hippocampus and amygdala to NAc spiny neurons (Harvey and Lacey, 1996; Groenewegen *et al*, 1999; Nicola *et al*, 2000). In order to understand how DA modulates amygdalar and hippocampal inputs to NAc neurons, we examined the effects of DArgic drugs on the responses evoked by selectively stimulating each of these inputs in an *in vitro* brain slice preparation optimized to enable the activation of each afferent system. A portion of this work has been published in abstract form (Charara and Grace, 2001).

MATERIALS AND METHODS

Tracer Injections-Light Microscopy

The courses of projection of hippocampal and amygdalar pathways to the NAc were analyzed using tracer injections to label afferent inputs. These studies were performed in male Sprague–Dawley rats weighing 250–300 g (Hilltop Laboratories, Scott-Dale, PA). Surgical procedures were carried out with animals under anesthesia with chloral hydrate (400 mg/kg, i.p.). All procedures were performed in accordance with the Guide for the Care and Use of Laboratory Animals published by the United States Public Health Services, with the experimental protocol approved by the University of Pittsburgh Institutional Animal Care and Use Committee. All efforts were made to minimize the number of animals used and their suffering.

In two rats (four hemispheres), bilateral injections of biocytin (4% in potassium acetate buffer; Sigma) were sterotaxically placed in the amygdala (coordinates with respect to bregma: AP −2.8 and −3.3 mm, ML +5.0 and +4.6 mm, and DV −8.4 mm) or subiculum (AP −5.0 and −5.3 mm from bregma; ML +0.9 and +1.2 mm, and DV −3.6 mm from the dura). The biocytin was iontophoretically delivered through glass micropipettes with a tip diameter ranging from 15 to 25 μm using 5 μA anodal current (7 s on, 7 s off) for 15–20 min. The animals were deeply anesthetized 48 h after the injection and perfused transcardially with 100 ml of Ringer's solution, followed by 300 ml of fixative containing 4% paraformaldehyde and 0.1% glutaraldehyde in phosphate buffer (PB; 0.1 M, pH 7.4). Free aldehydes were then removed by perfusion with 100 ml of 10% sucrose in 0.1 M PB. The brains were removed and stored in 30% sucrose solution until they sank. The fixed brains were then cut sagittally or horizontally with a freezing microtome into 80 μm-thick sections. After careful rinsing with phosphate-buffered saline (PBS; 0.05 M, pH 7.4), the sections were incubated for 12 h at 4°C in avidin-biotin-peroxidase complex (ABC 1:100; Vector labs) containing 0.3% Triton X-100 and 1% bovine serum albumin. After washing three times with PBS, the sections were incubated for 10 min in a mixture of diaminobenzidine (DAB) and H_2O_2. These sections were then mounted on gelatin-coated slides, air-dried, and a coverslip was applied with Permount. The sections were examined with bright field illumination using a Leitz microscope. For illustration purposes, the injection sites and the distribution of antergogradely labeled fibers were transferred onto standard drawings of the rat brain (Paxinos and Watson, 1986).

Electrophysiology

Intracellular recordings were made from medium spiny neurons in the slices as described previously (O'Donnell and Grace, 1993). Briefly, rats (male Sprague–Dawley, 200–300 g) were deeply anesthetized with chloral hydrate (400 mg/kg, i.p.) before transcardial perfusion with ice-cold physiological saline solution (229 mM sucrose, 1.9 mM KCl, 1.2 mM Na_2HPO_4, 33.3 mM $NaHCO_3$, 20 mM glucose, and 6 mM $MgCl_2$) oxygenated with a mixture of 95% O_2 and 5% CO_2. The brains were then quickly removed and 300 μm thick slices containing the NAc were cut either in the horizontal or sagittal plane using a vibratome, while submerged in the physiological saline solution. Slices containing the NAc were stored at least 1 h at room temperature in continuously oxygenated physiological saline (124 mM NaCl, 5 mM KCl, 1.2 mM KH_2PO_4, 2.4 mM $CaCl_2$, 1.3 mM $MgSO_4$, 26 mM $NaHCO_3$, and 10 mM glucose) saturated with 95%O_2 : 5% CO_2.

Intracellular recordings were performed using a submersion-type recording chamber (Warner Inst. Corp., RC-22) that was superfused (2 ml/min) with oxygenated physiological saline maintained at 34°C using a peristaltic pump (Haake-Büchler, MCP 2500). The time required for the complete exchange of media within the chamber was 3 min. Sharp electrodes were constructed from 1 mm OD Omegadot borosilicate glass tubing (World Precision Instruments, New Haven, CT) using a horizontal puller (Flaming-Brown P-80/PC). The electrodes were filled with 3.0 M potassium acetate or, in some cases, with 2% biocytin (Sigma, St Louis, MO) and had resistances of 55–100 MΩ measured *in situ*. Afferent fibers were stimulated using bipolar electrodes constructed from a pair of enamel-coated nichrome wires twisted together with the insulation at the tip removed to expose 0.5 mm of wire. Stimulation of afferent fibers was performed using 50 μA–1.2 mA constant current pulses that were 100–500 μs in duration. In order to stimulate the hippocampal and amygdaloid afferents innervating accumbal shell neurons, the electrode tips were placed gently on the surface of the slice in contact with the fornix and bed nucleus of the stria terminalis, respectively. The location of the recording site and the stimulating electrode were determined by visual inspection using a stereomicroscope (Nikon SMZ-2B), with the shell division of the NAc

identified according to the rat brain stereotaxic atlas of Paxinos and Watson (1986).

The electrodes were connected to the headstage of a NeuroData intracellular amplifier (Neurodata IR-183). Current was injected into neurons through a bridge circuit integral to the amplifier, with the current injection amplitude and the electrode voltage monitored on an oscilloscope (Kikusui COS5020-ST). Data were digitized using a NeuroData Neurorecorder (DR-886) and stored on VHS videotapes for subsequent off-line analysis. In addition, data were also digitized using a Microstar interface board prior to storage on a hard disk drive and off-line analysis. The analysis was performed using custom software (Neuroscope) running on a Windows-based PC computer. The input resistance was measured by injecting a series of hyperpolarizing constant current pulses of increasing amplitude (100–150 ms in duration) into the cell and measuring the resultant deflections in membrane potential.

All drugs were dissolved in the superfusion media and applied into the recording chamber. After obtaining stable baseline data and recording the responses to intracellular current injection and electrical stimulation of afferent fibers, the perfusion lines were switched from control to the drug-containing solutions, while maintaining stable perfusion pressure and fluid volume via the peristaltic pump delivery system. The drugs used were: DA (30–60 μM), SCH 23390 (3–5 μM), eticlopride (10 μM), SKF 38393 (10 μM), and quinpirole (10 μM). Ascorbic acid (0.02%) was added to the DA-containing solution to prevent oxidation of DA. To rule out any potential confounds related to the physiological actions of ascorbic acid, both control and DA-containing solutions contained the antioxidant. Since the time required for media exchange was 3 min, measurements of the drug effects were initiated following 1–2 min of exposure to drugs (ie 4–5 min after switching perfusion lines), at which point, a steady-state concentration of the drug in the chamber should have been achieved. The responses to the application of DA and DA agonists for a period of 1 min were similar to those observed after a prolonged application (3 min). Therefore, we chose 1–2 min of application to obtain a sufficient reproducibility of the response. Drug effects were evaluated by comparing the main peak value of EPSPs during the control (immediately before drug perfusion), drug application, and washout period (10–20 min). The statistical significance of drug-induced changes in measures of responses was determined using a paired Student's *t*-test.

RESULTS

Hippocampus-NAc pathway

In order to label most of the hippocampo-accumbal projections, two biocytin deposits were placed in the subiculum (Kelley and Domesick, 1982; Canteras and Swanson, 1992). This was performed to identify the course of fibers projecting to the NAc within the sagittal plane, since a considerable amount of the published anatomical data that described the topographical organization of the projections from the hippocampus to the NAc in rats was based on coronal sections (Kelley and Domesick, 1982; Groenewegen *et al*, 1987). The injection sites were confined to the subiculum and did not spread to adjacent areas (Figure 1a).

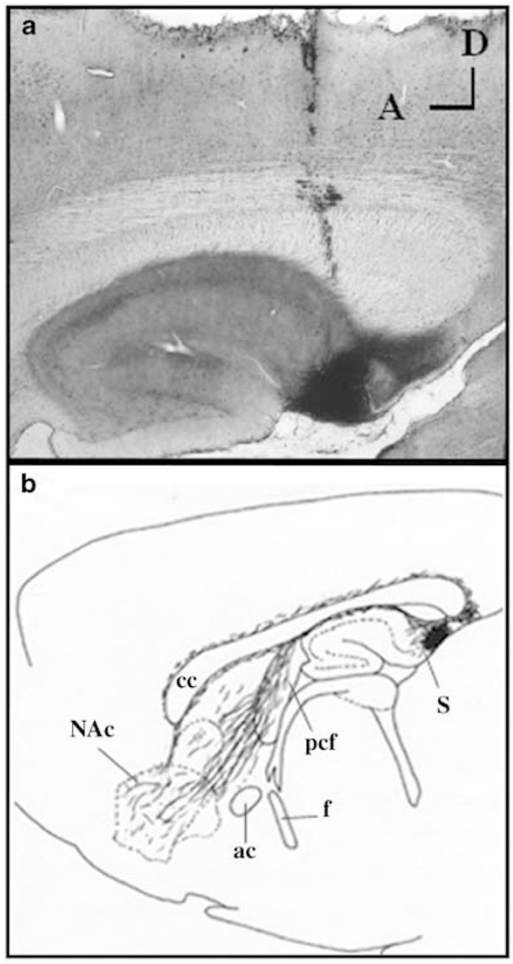

Figure 1 Hippocampal projection to the NAc. (a) Sagittal view of the rat hippocampus showing an injection site of biocytin in the subiculum. (b) A schematic drawing, in the sagittal plane, showing the pathway of biocytin-labeled fibers that leave the hippocampus and project to the NAc.

In a representative case, a major bundle of fibers is observed to arise from the injection site in the subiculum (Figure 1a, b). The fibers first enter the alveus, course dorsally and then run in the rostral direction through the fimbria/fornix. In the medial sections of the NAc, these fibers were seen to leave the postcommissural fornix en route to innervate the lateral septum and NAc as well as PFC, as described previously (Kelley and Domesick, 1982; Groenewegen *et al*, 1987; Jay and Witter, 1991). The fibers enter the NAc via the dorsal portion of the nucleus where they branch extensively, forming fine ramifications with varicosities, which probably represent axonal terminals. A schematic illustration of the course of the pathway is depicted in Figure 1. Thus, a sagittal plane of section was chosen to maximally preserve the hippocampal projection to the shell region of the NAc.

Amygdala-NAc Pathway

It is well known that the bulk of amygdalofugal projections terminating in the NAc take origin in the BLA and run

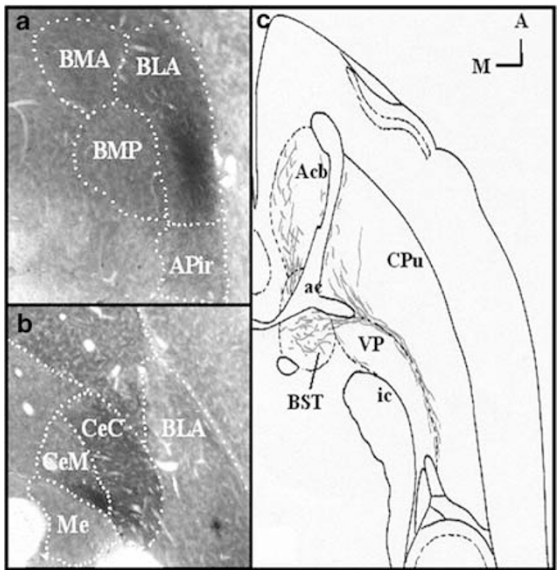

Figure 2 Amygdalar projection to the NAc. (a) and (b) are low power photomicrographs, in the horizontal plane, showing the injection sites of biocytin in the basolateral (a) and central (b) amygdala nuclei. (c) A schematic diagram of labeled fibers leaving the amygdala en route to the NAc.

through the stria terminalis (Kelley *et al*, 1982; McDonald, 1991). In an attempt to develop a brain slice preparation that preserves this amydala-accumbens pathway, horizontal and sagittal sections were tested. In one representative case, a large biocytin injection site was confined to the lateral part of the BLA (Figure 2a), although a smaller one could be seen in the central nucleus (Figure 2b). The biocytin deposits did not spread over adjacent areas. Pyramidal or piriform neurons with numerous dendrites were labeled around the injection site. From the injection site, labeled fibers extend in several directions, but for the present purpose, only those passing to the NAc and some adjoining subcortical structures were analyzed.

Over ventral sections, many amygdalofugal fibers traveled rostralward along the lateral edge of the ventral pallidum. From this bundle, fibers run through the ventral part of the NAc en route towards the olfactory bulb, although some of these fibers give off collaterals in the NAc and VP. Another major number of fibers exited the BLA and courses medially to join the stria terminalis. In more dorsal sections, fibers coursing through the stria terminalis reach the bed nucleus. Some of these fibers enter the medial part of the Nac, where they gave rise to thin branches bearing many large varicosities. A schematic illustration of the course of the pathway is depicted in Figure 2. Only horizontal sections are presented here since coronal and sagittal sections severed most of the amygdaloid fibers projecting to the NAc.

Membrane Properties and Morphology of Recorded Neurons

The data were collected from a total of 79 neurons that were located in the shell of the NAc, maintained a steady-state membrane potential greater than -55 mV, and had spike amplitudes greater than 60 mV. None of the cells exhibited spontaneous activity. However, spikes could be induced by injecting current pulses of 100–300 μs in duration and ranging from 0.1 to 0.7 nA. The resting membrane potential (RMP) ranged from -55 to -91 mV with a mean of -76 ± 2.4 mV (SEM; $n = 79$). The input resistance, estimated by injecting small amplitude hyperpolarizing current pulses (0.1–0.7 nA) and measuring the resultant membrane deflections, averaged 45.3 ± 1.4 MΩ ($n = 79$). The spike threshold, estimated by injection of depolarizing current pulses, averaged 42 ± 2.1 mV. The action potentials generated in response to the injection of the depolarizing current were 1.4 ± 0.2 ms in duration and 65 ± 1 mV in amplitude ($n = 79$). Inward rectification in the hyperpolarizing direction was present in 43 of the 79 neurons tested.

Overall, 26 out of 39 of the biocytin-filled neurons were identified as medium spiny projection neurons (Figure 3c). They had a soma diameter ranging from 13 to 21 μm and exhibited a variety of shapes: multipolar, oval, or fusiform. Three to five primary dendrites emerged from the cell body and the distal dendrites were covered with spines. The axons originated from the soma or from one of the primary dendrites and branched profusely within the dendritic field of the parent cell. The remaining neurons were not sufficiently labeled to clearly distinguish dendritic spines, but exhibited similar somatal size. The labeled neurons formed a sample of the total number of recorded neurons in the present study. The nonfilled cells exhibited similar physiological properties as those neurons identified mor-

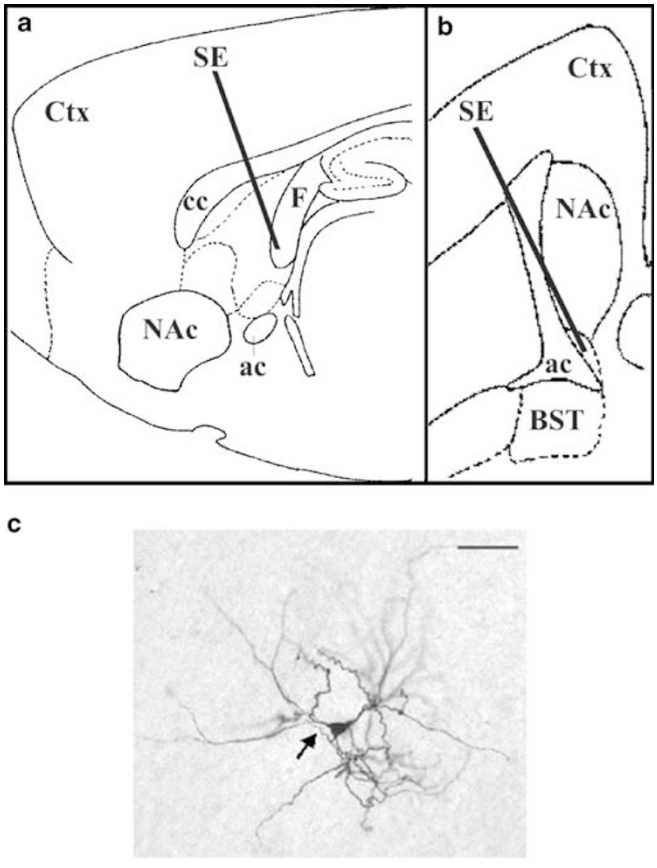

Figure 3 Line drawings illustrating the location of the stimulating electrodes in the fornix (a) and bed nucleus of stria terminalis (b). (c) A photomicrograph of an accumbens neuron that has been labeled by intracellular injection of biocytin following recording. The arrow indicates the axon emerging from the soma. Scale bar = 50 μm.

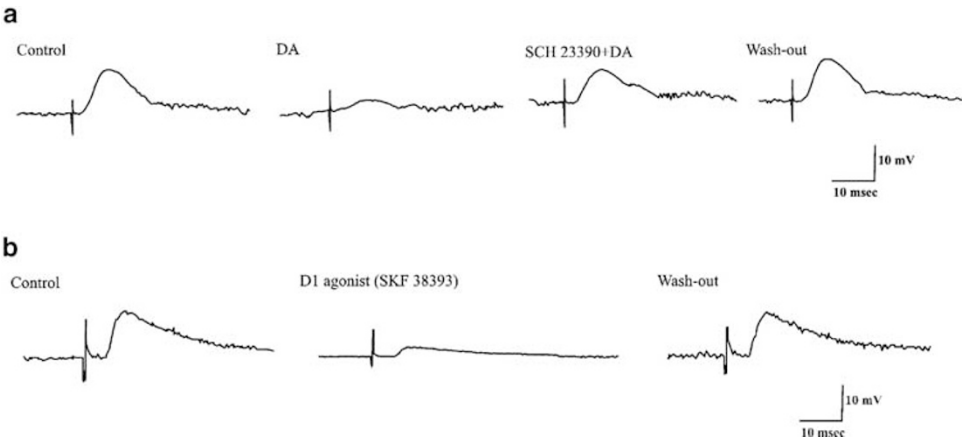

Figure 4 EPSPs evoked by fornix stimulation are attenuated by D1 receptor stimulation. (a) D1 receptor antagonist SCH 23390 (3 μM) partially reversed the DA (30 μM)-induced reduction of the EPSP evoked by hippocampal stimulation. (b) In another cell, the D1 receptor agonist SKF 38393 (10 μM) mimicked the effect of DA in that it attenuated the response to fimbria stimulation.

phologically as medium-sized spiny neurons after labeling with biocytin.

DA Effects on Membrane Properties of Nac Neurons

Previous studies have shown that DA application to NAc neurons produces three types of responses: that is, a biphasic response consisting of an initial hyperpolarization followed by a depolarization, and a monophasic response that was either hyperpolarizing or depolarizing in polarity (Uchimura *et al*, 1986). Similary, upon perfusion with DA (30–60 μM), the majority of NAc neurons tested in the present study (18 out of 35 cells) exhibited a membrane depolarization, although a few neurons exhibited either a membrane hyperpolarization (one out of 35) or a hyperpolarization followed by a depolarization (four out of 35). The remaining neurons were not affected. The membrane depolarization produced by DA ranged from 2 to 16 mV. These changes in membrane potential occurred without a corresponding change in the average input resistance, which was $45 \pm 2\,M\Omega$ in control conditions and $44 \pm 1.8\,M\Omega$ during perfusion with DA. However, in a subset of neurons (three out of 12), the depolarization was accompanied by an increase in input resistance ($46 \pm 1.1\,M\Omega$ in controls compared to $52 \pm 2\,M\Omega$ post-DA). These observations were consistent with our previous results (O'Donnell and Grace, 1996). Administration of the selective D1 agonist SKF 38393 (10 μM; $n = 27$) induced either a depolarization ($n = 11$) or an initial hyperpolarization and a subsequent depolarization ($n = 4$). On the other hand, administration of the selective D2 agonist quinpirole (10 μM) induced a hyperpolarization in six out of eight neurons tested. The remaining neurons were not affected. As observed with DA, in a subset of neurons, the depolarization was accompanied by an increase in input resistance (four out of 11), whereas the hyperpolarization was associated with a decrease in input resistance (three out of six).

DArgic Modulation of Hippocampal-Evoked Responses

When the rostro-ventral part of the fornix was stimulated electrically (Figure 3a), an excitatory postsynaptic potential (EPSP) was recorded in 29 of 35 neurons (Figures 4 and 5a, b). In the remaining portion of neurons, no response could be evoked. Increasing the amplitude of fiber stimulation caused a monotonic increase in the amplitude of EPSPs and was capable of driving action potentials in 17% (5/29) of neurons. In one cell, the EPSP was followed by an IPSP. The latency between the stimulus and the onset of the response averaged 4.1 ± 0.1 ms, with the EPSP reaching its peak amplitude of 10.7 ± 1.2 mV at 7 ms following the stimulus.

Perfusion with DA (30–60 μM) resulted in a significant reduction in the amplitude of the EPSP obtained by stimulation of the fornix (from 10.7 ± 1.2 to 4.5 ± 1.1 mV; $n = 12$, $p < 0.001$) (Figure 4, Table 1). The reduction of the EPSP amplitude was abolished by the D1 antagonist SCH 23390 (10 μm; 8.6 ± 1.1 mV compared to control; $p < 0.001$; $n = 7$; 3–5 μM), but not by the D2 antagonist eticlopride

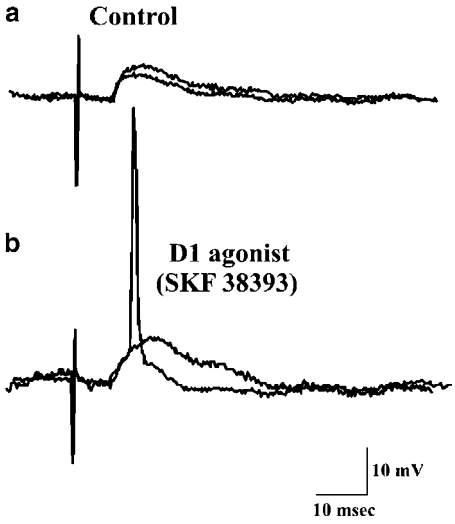

Figure 5 In 13% of the neurons tested, D1 receptor stimulation facilitated fornix-evoked responses. (a) Overlay of two responses evoked in a NAc neuron after stimulation of the fimbria with 800 and 1000 μA current pulses (300 ms duration). (b) The D1 receptor agonist SKF 38393 (10 μM) caused an increase in the amplitude of the evoked EPSPs in comparison to control, after stimulation of the fimbria with the same current intensities.

Table 1 Effects of DA receptor agonists on EPSP peak amplitude after fornix stimulation and after stimulation of the bed nucleus of the stria terminalis

	Dopamine ($n=12$)	D1 agonist ($n=12$)	D2 agonist ($n=5$)
After fornix stimulation			
Control	10.7 ± 1.2 mV	10.3 ± 1.8 mV	9.7 ± 1.4 mV
Drug	4.5 ± 1.1 mV*	3.2 ± 1.3 mV*	9.7 ± 1.2 mV
After stimulation of the bed nucleus of the stria terminalis			
	Dopamine ($n=10$)	D1 agonist ($n=11$)	D2 agonist ($n=4$)
Control	8.4 ± 1.5 mV	8.6 ± 1.7 mV	8.5 ± 1.3 mV
Drug	2.1 ± 1.2 mV*	3.5 ± 1.1 mV*	6.4 ± 1.2 mV

Paired student's *t*-test; $p<0.001$.*Statistical significance was determined by comparing drug values with predrug control values using a paired *t*-test, $p<0.001$.

(10 μm; 10.1 ± 1.3 mV; $n=5$; 10 μM). In another subset of neurons ($n=12$), the D1 agonist SKF 38393 (10 μM) reduced the EPSP amplitude in a similar manner as that induced by DA (from 10.3 ± 1.8 to 3.2 ± 1.3 mV; $p<0.001$). In contrast, administration of moderately high doses of the D2 agonist quinpirole (10 μM) failed to induce changes in EPSP amplitude (9.7 ± 1.4 mV compared to 9.7 ± 1.2 mV; $p>0.01$; $n=5$; Table 1). The neurons returned to near baseline conditions following perfusion with a drug-free solution for 10–20 min (Figures 4 and 7a).

In 14% (4/29) of the neurons, the administration of the D1 agonist SKF 38393 (10 μM) induced an increase in the amplitude of the fornix-evoked EPSPs when compared to control (10.2 ± 1.2 mV in control; 12.3 ± 1 mV in the presence of D1 agonist; $p<0.01$; $n=4$) with the same current intensities (Figure 5a, b). In one of the cells (1/4), the presence of D1 agonist SKF 38393 (10 μM) enabled fornix stimulation to evoke spike discharge following the high intensity stimulus (Figure 5b), whereas stimulation was incapable of evoking spike discharge prior to SKF 38393 administration.

DArgic Modulation of Amygdala-Evoked Responses

Overall, stimulation of basolateral amygdaloid afferents located in the bed nucleus of the stria terminalis (Figure 3b) evoked EPSPs in 25 out of 38 neurons studied. The latency for the EPSP onset averaged 4.2 ± 0.2 ms. Increasing the amplitude of afferent stimulation was capable of evoking spikes in only 8% (2/25) of the neurons that responded to the stimulation.

Bath application of DA (30 μM) attenuated the amplitude of EPSPs evoked in accumbal neurons following stimulation of the bed nucleus of stria terminalis (8.4 ± 1.5–2.1 ± 1.2 mV; $n=10$) (Figure 6; Table 1). Administration of the D1 antagonist SCH 23390 ($n=6$; 3–5 μM) attenuated the effect of DA (6.5 ± 1.3 mV; $p<0.001$), whereas the D2 antagonist eticlopride (10 μM) was ineffective (8.1 ± 1.1 mV compared to control; $n=4$). In another subset of neurons ($n=11$), the D1 agonist SKF 38393 (10 μM) reduced the EPSP amplitude in a similar manner as with DA (8.6 ± 1.7–3.5 ± 1.1 mV; $p<0.001$) (Figure 6, Table 1). Administration of the D2 agonist quinpirole (10 μM; $n=3$) failed to induce substantial changes in EPSP amplitude (8.5 ± 1.3 mV compared to 6.4 ± 1.2 mV) (Table 1). As was the case for hippocampal stimulation, the neurons returned to near baseline conditions following perfusion with a drug-free solution for 10–20 min (Figure 7b).

DISCUSSION

The major finding of this study was that D1 receptor activation depressed the excitatory postsynaptic responses of the majority of NAc neurons recorded during stimulation of hippocampal and amygdaloid afferents. In a small population of NAc cells (14%), however, D1 stimulation induced a facilitation of the hippocampus-evoked response. In contrast to results with prefrontal cortical afferent stimulation (O'Donnell and Grace, 1994), D2 stimulation did not attenuate the EPSP amplitude evoked from either the amygdala or hippocampus afferent system. Altogether, these observations indicate a DA receptor subtype-specific modulation of glutamatergic inputs to the NAc, with D2 agonists attenuating PFC drive (O'Donnell and Grace, 1994), and D1 agonists attenuating BLA drive, but with hippocampal-evoked responses showing a bimodal form of modulation by D1 stimulation.

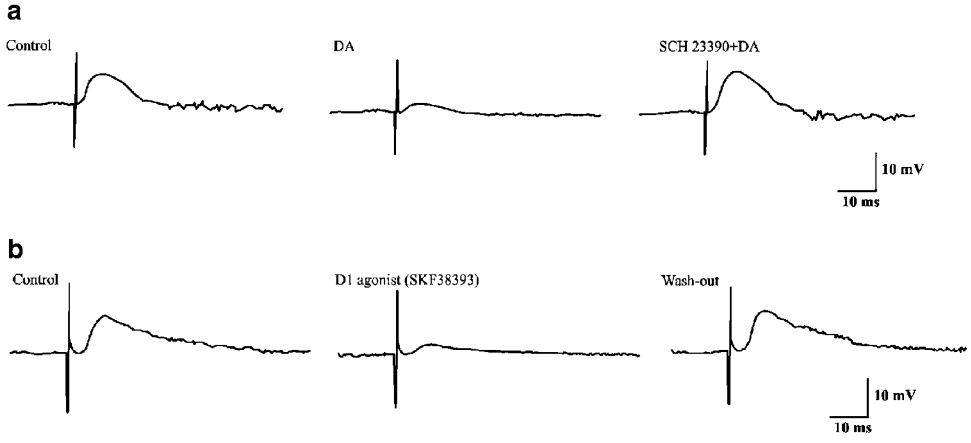

Figure 6 D1 receptor stimulation attenuates amygdala-evoked responses. (a) D1 receptor antagonist SCH 23390 (3 μM) partially reversed the DA (30 μM)-induced reduction of the EPSP evoked by electrical stimulation of the bed nucleus of stria terminalis. (a) In another cell, the D1 receptor agonist SKF 38393 (10 μM) mimicked the effect of DA in that it attenuated the response to amygdaloid fiber stimulation.

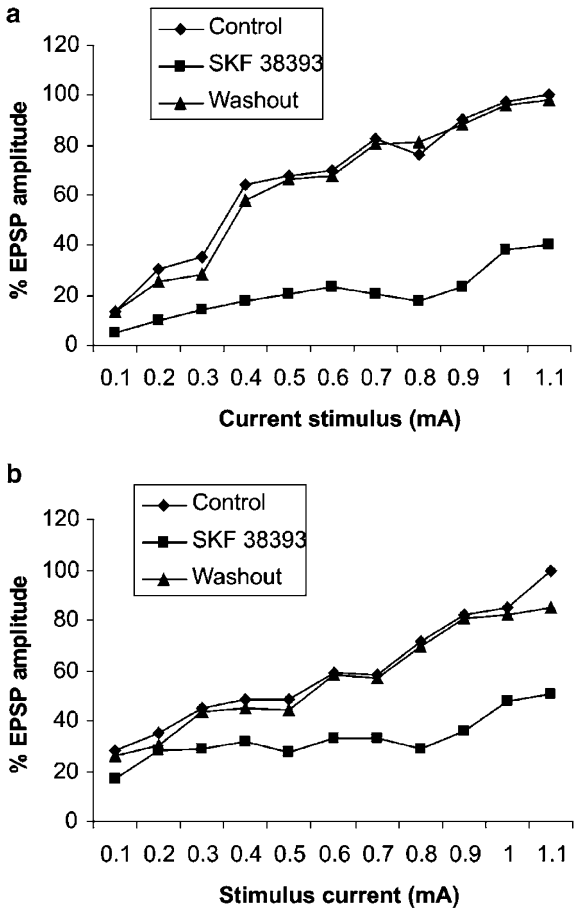

Figure 7 DA effects on NAc postsynaptic responses. (a) Representative curve of the excitatory postsynaptic responses recorded and averaged in NAc neurons after stimulation of the fornix before, during, and after application of the D1 agonist SKF 38393. (b) Representative graph of the excitatory postsynaptic responses recorded and averaged in NAc neurons after stimulation of the bed nucleus of stria terminalis, before, during, and after application of the D1 agonist SKF 38393. In both the cases (a, b), the EPSPs show a steep rise in amplitude between 0.2 and 0.3 mA and a gradual saturation close to 1.1 mA. During the application of D1 agonist SKF 38393, the EPSP is attenuated for all intensities tested.

NAc Neurons and DA Effects

Overall, the electrophysiological properties of NAc neurons recorded in this study were similar to those described previously using *in vitro* intracellular recordings (Chang and Kitai, 1986; Uchimura *et al*, 1986, 1989; Pennartz and Kitai, 1991; O'Donnell and Grace, 1993). These properties correspond to those of NAc medium spiny projection neurons (Chang and Kitai, 1985; Pennartz *et al*, 1992a; O'Donnell and Grace, 1993). Perfusion of NAc slices with DA induced a reversible depolarization in most of the neurons tested without changing their input resistance. However, some neurons exhibited either a hyperpolarization or an initial hyperpolarization followed by a depolarization. The administration of the selective D1 agonist induced either a depolarization or an initial hyperpolarization and a subsequent depolarization, whereas administration of the selective D2 agonist induced only a hyperpolarization. These results suggest that the hyperpolarizing and depolarizing actions of DA on NAc neurons are exerted via different DA receptor subtypes. Our findings are consistent with the DA-induced effects observed in previous studies in NAc neurons (Uchimura *et al*, 1986; O'Donnell and Grace, 1994). However, the exact mechanism underlying the changes observed remains to be established.

Effects of D1-Like Receptor Activation on Excitatory Postsynaptic Responses

The synaptic responses recorded in NAc shell neurons in response to amygdaloid and hippocampal afferent activation were attenuated by DA in the majority of the cases, although 14% of the NAc neurons increased EPSP amplitude following fornix stimulation and D1 application. Our results argue strongly that the depressant actions of DA occurred via an action at D1 receptors. Thus, the DA-induced attenuation was substantially blocked by the D1 antagonist SCH 233390, but not by the D2 receptor antagonist eticlopride. Moreover, the selective D1 receptor agonist SKF 38393, but not the D2 receptor agonist quinpirole, mimicked the effects of DA on EPSP amplitude. Consistent with our findings, when stimulating nonidentified afferent fiber bundles *in vitro*, many other investigators also observed a D1-like receptor-mediated decrease in EPSP amplitude (Higashi *et al*, 1989; Pennartz *et al*, 1992b; Harvey and Lacey, 1996, 1997; Nicola *et al*, 1996; Nicola and Malenka 1997, 1998). *In vivo*, VTA stimulation or inotophoretically applied DA was found to depress NAc neuron firing evoked by stimulation of the amygdala (Yim and Mogenson, 1982, 1986, 1989) or hippocampus (DeFrance *et al*, 1985; Yang and Mogenson, 1984, 1986). The finding that D1 antagonist administration did not increase amplitude beyond the predrug baseline suggests that these D1 receptors are not under tonic stimulation *in vitro*, as found for D2 receptor antagonist actions on PFC afferents (O'Donnell and Grace, 1994).

Our findings that D1 application increases the amplitude of the synaptic response evoked by fornix stimulation in a small population of neurons is in agreement with a recent *in vivo* study showing a D1-mediated potentiation of hippocampus-evoked spike firing activity (Floresco *et al*, 2001a). One of several potential reasons for the facilitatory D1 effect is the enhancement of postsynaptic glutamate receptor responsiveness, in particular those mediated by *N*-methyl-D-aspartate (NMDA) receptors (Cepeda *et al*, 1993; Umemiya and Raymond, 1997). In contrast, studies of Yang and Mogenson (1986) suggested the presence of D2-mediated presynaptic effect of DA on these terminals. Whether this is due to differences between *in vivo*/*in vitro* preparations or the interactions of D2 drugs with other afferent processes known to be attenuated by D2 receptors (eg PFC-NAc fibers) is unclear.

Mechanism and Site of Action of D1 Receptor Stimulation in the NAc

The mechanism by which DA D1 receptor activation depresses excitatory transmission evoked in the NAc following stimulation of glutamatergic afferents is the subject of some controversy. The majority of *in vitro* studies have suggested that the D1 receptor-mediated reduction in EPSP amplitude appears to be a presynaptic

effect because the paired-pulse facilitation is increased by DA (Pennartz *et al*, 1992b; Nicola *et al*, 1996) and DA reduces the frequency of spontaneous miniature EPSCs (Nicola *et al*, 1996). However, anatomical findings do not support the existence of presynaptic D1 receptors on glutamate terminals in the NAc (Yung *et al*, 1995). A second proposed mechanism is based on the finding that adenosine A1 receptor antagonists block the effects of DA on EPSPs and that postsynaptic D1 receptor activation increases synaptic NMDA-mediated responses *in vitro* (Harvey and Lacey, 1997). The authors conclude that the enhanced current flow through the NMDA receptor promotes the production of adenosine that acts as a retrograde trans-synaptic messenger to presynaptically inhibit glutamate release. Floresco *et al* (2001b) found similar results in which the administration of either D1 or adenosine antagonists blocked the DA-mediated inhibition of BLA-evoked spiking activity *in vivo*. This hypothesis is consistent with the anatomical localization of D1 receptors on postsynaptic dendritic spines and shafts of striatal neurons and NAc cells (Huang *et al*, 1992; Levey *et al*, 1993; Hersch *et al*, 1995; Yung *et al*, 1995; Caille *et al*, 1996). However, this interpretation has been challenged by Nicola and Malenka (1997), who were unable to replicate the findings that A1 or NMDA receptor antagonists block the DA-induced depression of excitatory synaptic transmission and thus concluded that presynaptic D1 receptors are responsible for this effect. Nonetheless, when considered at the level of DA modulation of interacting systems, our results are consistent in showing a D1-mediated attenuation of amygdaloid and hippocampal afferent inputs to NAc neurons.

Functional Implications

DA plays a complex role in the gating of afferent input to the NAc, in a manner that depends on the current state of the system. The hippocampal pathway to the NAc has been implicated in exploratory and goal-directed locomotion (Yang and Mogenson, 1987; Burns *et al*, 1996; Floresco *et al*, 1997; Bannerman *et al*, 2001), whereas the amygdala-NAc pathway is believed to play an essential role in mediating affect-facilitation of memory storage (Roozendaal *et al*, 2001) and approach to conditioned stimuli (Everitt *et al*, 1991). DA neurotransmission may gate responses of the NAc to particular inputs that in turn may facilitate appropriate behavioral response selection in complex rewarding situations (Mogenson *et al*, 1993; Floresco *et al*, 2001a, b). Our previous *in vitro* and *in vivo* studies showed that the tonic levels of extracellular DA are sufficient to partially attenuate at least 60% of PFc afferents to the striatal complex, since administration of a D2 antagonist increases the amplitude of the PFC-evoked response when administered alone (O'Donnell and Grace, 1994; West and Grace, 2002). This was not observed with the D1 antagonist. Given these data, it would appear that enhanced DA neurotransmission can selectively gate afferent interactions in this region. Thus, if DA activation of D2 receptors is actively suppressed or blocked by a D2 antagonist, the input from the PFC would be selectively potentiated relative to hippocampal and amygdaloid inputs. At basal DA levels, stimulation of D2 receptors would attenuate PFc input without inhibiting the hippocampal and amygdaloid afferents (O'Donnell and Grace, 1994), thus shifting the balance toward these subcortical limbic structures. However, with activation of the DA system, increased DA transmission would attenuate most afferent hippocampal and amygdaloid input. The one exception would be its ability to augment a subset of hippocampal-NAc afferents. Given our studies showing that hippocampal/subicular activation will tonically augment VTA DA population activity (Floresco *et al*, 2001c), such a selective facilitation of an ensemble of hippocampal afferents by D1 receptor activation would permit the hippocampus to have a dominant influence over behavior during periods of exploration (Floresco and Phillips, 1999). In addition, considering that the hippocampus can also facilitate PFc inputs to the NAc (O'Donnell and Grace, 1995), it is possible that facilitation of hippocampal input to the NAc could in turn lead to selective gating of PFc inputs on the same neuron, offsetting the D2-mediated inhibition of this pathway. Thus, during periods of enhanced DA efflux, hippocampal inputs conveying contextual information about the environment could permit a selective gating of PFc inputs which can lead to specific patterns of behavior that are appropriate to that context.

ACKNOWLEDGEMENTS

This work was supported by United States Public Health Service Grants MH, 45156, 57440 (AAG) and National Alliance for Research on Schizophrenia and Depression (AC). We thank Dr Hank Jedema for his help with the *in vitro* slice recordings. We also thank Nicole MacMurdo and Christy Wyant for their technical assistance, and Brian Lowry for the development of software (Neuroscope) used in data acquisition. We are grateful to Drs Holly Moore, Stan Floresco and Anthony West for their valuable comments, suggestions, and enlightening discussions regarding this manuscript.

REFERENCES

Alvarez P, Zola-Morgan S, Squire LR (1995). Damage limited to the hippocampal region produces long-lasting memory impairment in monkeys. *J Neurosci* **15**: 3796–3807.

Bannerman DM, Gilmour G, Norman G, Lemaire M, Iversen SD, Rawlins JN (2001). The time course of the hyperactivity that follows lesions or temporary inactivation of the fimbria-fornix. *Behav Brain Res* **120**: 1–11.

Berendse HW, Groenewegen HJ (1990). Organization of the thalamostriatal projections in the rat, with special emphasis on the ventral striatum. *J Comp Neurol* **299**: 187–228.

Bouyer JJ, Joh TH, Pickel VM (1984). Ultrastructural localization of tyrosine hydroxylase in rat nucleus accumbens. *J Comp Neurol* **227**: 92–103.

Burns LH, Annett L, Kelley AE, Everitt BJ, Robbins TW (1996). Effects of lesions to amygdala, ventral subiculum, medial prefrontal cortex, and nucleus accumbens on the reaction to novelty: implication for limbic-striatal interactions. *Behav Neurosci* **110**: 60–73.

Caille I, Dumartin B, Bloch B (1996). Ultrastructural localization of D1 dopamine receptor immunoreactivity in rat striatonigral neurons and its relation with dopaminergic innervation. *Brain Res* **730**: 17–31.

Callaway CW, Hakan RL, Henriksen SJ (1991). Distribution of amygdala input to the nucleus accumbens septi: an electrophysiological investigation. *J Neural Transm* **83**: 215–225.

Canteras NS, Swanson LW (1992). Projections of the ventral subiculum to the amygdala, septum, and hypothalamus: a PHAL anterograde tract-tracing study in the rat. *J Comp Neurol* **324**: 180–194.

Chang HT, Kitai ST (1986). Intracellular recordings from rat nucleus accumbens neurons *in vitro*. *Brain Res* **366**: 392–396.

Charara A, Grace AA (2001). Mesolimbic dopamine modulates hippocampus- and amygdala evoked responses in rat nucleus accumbens: an *in vitro* study. *Soc Neurosci Abstr* **27**: 918.9.

Cepeda C, Buchwald NA, Levine MS (1993). Neuromodulatory actions of dopamine in the neostriatum are dependent upon the excitatory amino acid receptor subtypes activated. *Proc Natl Acad Sci USA* **90**: 9576–9580.

Chang HT, Kitai ST (1985). Projection neurons of the nucleus accumbens: an intracellular labeling study. *Brain Res* **347**: 112–116.

Davis M (1992). The role of the amygdala in fear and anxiety. *Annu Rev Neurosci* **15**: 353–375.

DeFrance JF, Marchand JF, Sikes RW, Chronister RB, Hubbard JI (1985). Charcaterization of fimbria input to nucleus accumbens. *J Neurophysiol* **54**: 1553–1567.

Descarries L, Watkins KC, Garcia S, Bosler O, Doucet G (1996). Dual character, asynaptic and synaptic, of the dopamine innervation in adult rat neostriatum: a quantitative autoradiographic and immunocytochemical analysis. *J Comp Neurol* **375**: 167–186.

Everitt BJ, Morris KA, O'Brien A, Robbins TW (1991). The basolateral amygdala-ventral striatal system and conditioned place preference: further evidence of limbic-striatal interactions underlying reward-related processes. *Neuroscience* **42**: 1–18.

Finch DM (1996). Neurophysiology of converging synaptic inputs from the rat prefrontal cortex, amygdala, midline thalamus, and hippocampal formation onto single neurons of the caudate/putamen and nucleus accumbens. *Hippocampus* **6**: 495–512.

Floresco SB, Blaha CD, Yang CR, Phillips AG (2001a). Modulation of hippocampal and amygdalar-evoked activity of nucleus accumbens neurons by dopamine: cellular mechanisms of input selection. *J Neurosci* **21**: 2851–2860.

Floresco SB, Blaha CD, Yang CR, Phillips AG (2001b). Dopamine D1 and NMDA receptors mediate potentiation of basolateral amygdala-evoked firing of nucleus accumbens neurons. *J Neurosci* **21**: 6370–6376.

Floresco SB, Phillips AG (1999). Dopamine and hippocampal input to the nucleus accumbens play an essential role in the search for food in an unpredictable environment. *Psychobiology* **27**: 277–286.

Floresco SB, Seamans JK, Phillips AG (1997). Selective roles for hippocampal, prefrontal cortical, and ventral striatal circuits in radial-arm maze tasks with or without a delay. *J Neurosci* **17**: 1880–1890.

Floresco SB, Todd CL, Grace AA (2001c). Glutamatergic afferents from the hippocampus to the nucleus accumbens regulate activity of ventral tegmental area dopamine neurons. *J Neurosci* **21**: 4915–4922.

Garris PA, Ciolkowski EL, Pastore P, Wightman RM (1994). Efflux of dopamine from the synaptic cleft in the nucleus accumbens of the rat brain. *J Neurosci* **14**: 6084–6093.

Grace AA (1991). Phasic versus tonic dopamine release and the modulation of dopamine system responsivity: a hypothesis for the etiology of schizophrenia. *Neuroscience* **41**: 1–24.

Groenewegen HJ, Vermeulen-Van der Zee E, te Kortschot A, Witter MP (1987). Organization of the projections from the subiculum to the ventral striatum in the rat. A study using anterograde transport of Phaseolus vulgaris leucoagglutinin. *Neuroscience* **23**: 103–120.

Groenewegen HJ, Wright CI, Beijer AV, Voorn P (1999). Convergence and segregation of ventral striatal inputs and outputs. *Ann NY Acad Sci* **877**: 49–63.

Harvey J, Lacey MG (1996). Endogenous and exogenous dopamine depress EPSCs in rat nucleus accumbens *in vitro* via D1 receptor activation. *J Physiol* **492**: 143–154.

Harvey J, Lacey MG (1997). A postsynaptic interaction between dopamine D1 and NMDA receptors promotes presynaptic inhibition in the rat nucleus accumbens via adenosine release. *J Neurosci* 175271–175280.

Heimer L, Alheid GF (1991). Piecing together the puzzle of basal forebrain anatomy. *Adv Exp Med Biol* **295**: 1–42.

Hersch SM, Ciliax BJ, Gutekunst CA, Rees HD, Heilman CJ, Yung KK *et al* (1995). Electron microscopic analysis of D1 and D2 dopamine receptor proteins in the dorsal striatum and their synaptic relationships with motor corticostriatal afferents. *J Neurosci* **15**: 5222–5237.

Higashi H, Inanaga K, Nishi S, Uchimura N (1989). Enhancement of dopamine actions on rat nucleus accumbens neurones *in vitro* after methamphetamine pre-treatment. *J Physiol* **408**: 587–603.

Huang Q, Zhou D, Chase K, Gusella JF, Aronin N, DiFiglia M (1992). Immunohistochemical localization of the D1 dopamine receptor in rat brain reveals its axonal transport, pre- and postsynaptic localization, and prevalence in the basal ganglia, limbic system, and thalamic reticular nucleus. *Proc Natl Acad Sci USA* **89**: 11988–11992.

Hyman SE (1996). Addiction to cocaine and amphetamine. *Neuron* **16**: 901–904.

Iversen SD (1995). Interactions between excitatory amino acids and dopamine systems in the forebrain: implications for schizophrenia and Parkinson's disease. *Behav Pharmacol* **6**: 478–491.

Jay TM, Witter MP (1991). Distribution of hippocampal CA1 and subicular efferents in the prefrontal cortex of the rat studied by means of anterograde transport of Phaseolus vulgaris-leucoagglutinin. *J Comp Neurol* **313**: 574–586.

Kalivas PW, Sorg BA, Hooks MS (1993). The pharmacology and neural circuitry of sensitization to psychostimulants. *Behav Pharmacol* **4**: 315–334.

Kelley AE, Domesick VB (1982). The distribution of the projection from the hippocampal formation to the nucleus accumbens in the rat: an anterograde- and retrograde-horseradish peroxidase study. *Neuroscience* **7**: 2321–2335.

Kelley AE, Domesick VB, Nauta WJ (1982). The amygdalostriatal projection in the rat—an anatomical study by anterograde and retrograde tracing methods. *Neuroscience* **7**: 615–630.

Lavin A, Grace AA (1994). Modulation of dorsal thalamic cell activity by the ventral pallidum: its role in the regulation of thalamocortical activity by the basal ganglia. *Synapse* **18**: 104–127.

LeDoux JE (1993). Emotional memory systems in the brain. *Behav Brain Res* **58**: 69–79.

Levey AI, Hersch SM, Rye DB, Sunahara RK, Niznik HB, Kitt CA *et al* (1993). Localization of D1 and D2 dopamine receptors in brain with subtype-specific antibodies. *Proc Natl Acad Sci USA* **90**: 8861–8865.

McDonald AJ (1991). Topographical organization of amygdaloid projections to the caudate putamen, nucleus accumbens, and related striatal-like areas of the rat brain. *Neuroscience* **44**: 15–33.

Mogenson GJ, Brudzynski SM, Wu M, Yang CR, Yim CY (1993). From motivation to action: a review of dopamine regulation of limbic-nucleus accumbens-ventral pallidum-pedunculopontine nucleus circuitries involved in limbic-motor integration. In: Kalivas PW, Barnes CD (eds) *Limbic Motor Circuits and Neuropsyciatry*. CRC Press: Boca Raton, FL. pp 193–236.

Mulder AB, Hodenpijl MG, Lopes da Silva FH (1998). Electrophysiology of hippocampal and amygdaloid projections to the

nucleus accumbens of the rat: convergence, segregation, and interaction of inputs. *J Neurosci* **18**: 5095–5102.

Nauta WJ, Smith GP, Faull RL, Domesick VB (1978). Efferent connections and nigral afferents of the nucleus accumbens septi in the rat. *Neuroscience* **3**: 385–401.

Nicola SM, Kombian SP, Malenka RC (1996). Psychostimulants depress excitatory synaptic transmission in the nucleus accumbens via presynaptic D1-like dopamine receptors. *J Neurosci* **16**: 1591–1604.

Nicola SM, Malenka RC (1997). Dopamine depresses excitatory and inhibitory synaptic transmission by distinct mechanisms in the nucleus accumbens. *J Neurosci* **17**: 5697–5710.

Nicola SM, Malenka RC (1998). Modulation of synaptic transmission by dopamine and norepinephrine in ventral but not dorsal striatum. *J Neurophysiol* **79**: 1768–1776.

Nicola SM, Surmeier J, Malenka RC (2000). Dopaminergic modulation of neuronal excitability in the striatum and nucleus accumbens. *Annu Rev Neurosci* **23**: 185–215.

O'Donnell P, Grace AA (1993). Physiological and morphological properties of accumbens core and shell neurons recorded *in vitro*. *Synapse* **13**: 135–160.

O'Donnell P, Grace AA (1994). Tonic D2-mediated attenuation of cortical excitation in nucleus accumbens neurons recorded *in vitro*. *Brain Res* **634**: 105–112.

O'Donnell P, Grace AA (1995). Synaptic interactions among excitatory afferents to nucleus accumbens neurons: hippocampal gating of prefrontal cortical input. *J Neurosci* **15**: 3622–3639.

O'Donnell P, Grace AA (1996). Dopaminergic reduction of excitability in nucleus accumbens neurons recorded *in vitro*. *Neuropsychopharmacology* **15**: 87–97.

Paxinos G, Watson C 1986. *The Rat Brain in Stereotaxic Coordinates*. Academic Press: New York.

Pennartz CM, Dolleman-van Der Weel MJ, Kitai ST, Lopes da Silva FH (1992a). Differential membrane properties and dopamine effects in the shell and core of the rat nucleus accumbens studied *in vitro*. *Neurosci Lett* **136**: 109–112.

Pennartz CM, Dolleman-van Der Weel MJ, Kitai ST, Lopes da Silva FH (1992b). Presynaptic dopamine D1 receptors attenuate excitatory and inhibitory limbic inputs to the shell region of the rat nucleus accumbens studied *in vitro*. *J Neurophysiol* **67**: 1325–1334.

Pennartz CM, Groenewegen HJ, Lopes da Silva FH (1994). The nucleus accumbens as a complex of functionally distinct neuronal ensembles: an integration of behavioural, electrophysiological and anatomical data. *Prog Neurobiol* **42**: 719–761.

Pennartz CM, Kitai ST (1991). Hippocampal inputs to identified neurons in an *in vitro* slice preparation of the rat nucleus accumbens: evidence for feed-forward inhibition. *J Neurosci* **11**: 2838–2847.

Robbins TW, Everitt BJ (1996). Neurobehavioural mechanisms of reward and motivation. *Curr Opin Neurobiol* **6**: 228–236.

Roozendaal B, de Quervain DJ, Ferry B, Setlow B, McGaugh JL (2001). Basolateral amygdala-nucleus accumbens interactions in mediating glucocorticoid enhancement of memory consolidation. *J Neurosci* **21**: 2518–2525.

Sesack SR, Deutch AY, Roth RH, Bunney BS (1989). Topographical organization of the efferent projections of the medial prefrontal cortex in the rat: an anterograde tract-tracing study with Phaseolus vulgaris leucoagglutinin. *J Comp Neurol* **290**: 213–242.

Sesack SR, Pickel VM (1990). In the rat medial nucleus accumbens, hippocampal and catecholaminergic terminals converge on spiny neurons and are in apposition to each other. *Brain Res* **527**: 266–279.

Sesack SR, Pickel VM (1992). Prefrontal cortical efferents in the rat synapse on unlabeled neuronal targets of catecholamine terminals in the nucleus accumbens septi and on dopamine neurons in the ventral tegmental area. *J Comp Neurol* **320**: 145–160.

Uchimura N, Higashi H, Nishi S (1986). Hyperpolarizing and depolarizing actions of dopamine via D-1 and D-2 receptors on nucleus accumbens neurons. *Brain Res* **375**: 368–372.

Uchimura N, Higashi H, Nishi S (1989). Membrane properties and synaptic responses of the guinea pig nucleus accumbens neurons *in vitro*. *J Neurophysiol* **61**: 769–779.

Umemiya M, Raymond LA (1997). Dopaminergic modulation of excitatory postsynaptic currents in rat neostriatal neurons. *J Neurophysiol* **78**: 1248–1255.

West AR, Grace AA (2002). Opposite influences of endogenous dopamine D1 and D2 receptor activation on activity states and electrophysiological properties of striatal neurons: studies combining *in vivo* intracellular recordings and reverse microdialysis. *J Neurosci* **22**: 294–304.

Yang CR, Mogenson GJ (1984). Electrophysiological responses of neurons in the nucleus accumbens to hippocampal stimulation and the attenuation of the excitatory responses by the mesolimbic dopaminergic system. *Brain Res* **324**: 69–84.

Yang CR, Mogenson GJ (1986). Dopamine enhances terminal excitability of hippocampal-accumbens neurons via D2 receptor: role of dopamine in presynaptic inhibition. *J Neurosci* **6**: 2470–2478.

Yang CR, Mogenson GJ (1987). Hippocampal signal transmission to the pedunculopontine nucleus and its regulation by dopamine D2 receptors in the nucleus accumbens: an electrophysiological and behavioural study. *Neuroscience* **23**: 1041–1055.

Yim CH, Mogenson GJ (1982). Response of nucleus accumbens neurons to amygdala stimulation and its modification by dopamine. *Brain Res* **239**: 401–415.

Yim CH, Mogenson GJ (1986). Mesolimbic dopamine projection modulates amygdala-evoked EPSP in nucleus accumbens neurons: an *in vivo* study. *Brain Res* **369**: 347–352.

Yim CH, Mogenson GJ (1989). Low doses of accumbens dopamine modulate amygdala suppression of spontaneous exploratory activity in rats. *Brain Res* **477**: 202–210.

Yung KK, Bolam JP, Smith AD, Hersch SM, Ciliax BJ, Levey AI (1995). Immunocytochemical localization of D1 and D2 dopamine receptors in the basal ganglia of the rat: light and electron microscopy. *Neuroscience* **65**: 709–730.